Feasibility of a mitral annuloplasty with the capability for peri- and post-operative adjustment

Abstract

Surgical repair with implantation of a mitral annuloplasty ring is the gold standard treatment for mitral regurgitation. However, outcomes are variable and recurrent mitral regurgitation is not uncommon. A REshapeable Mitral Annuloplasty DevIce (REMADI) is proposed, which consists of a fully encapsulated low melting temperature alloy. The alloy is solid and rigid at body temperature and provides traction force to shape the annulus. When heated using a non-contact method, the alloy melts and the REMADI becomes malleable. The REMADI is engaged with the mitral valve annulus using anchors which automatically deploy upon contact. A passive beating porcine heart model was used to demonstrate the feasibility of the REMADI device, which was deployed, engaged, and used to reduce the diameter of the mitral valve annulus.

Introduction

Mitral regurgitation (MR) is a debilitating disease which affects 2% of the European adult population, with 250,000 new patients diagnosed worldwide per year [1]. MR is the predominant valvular pathology in Western populations, with an incidence which increases rapidly with age [2]. In the UK, 2,929 primary surgical mitral valve procedures were performed in 2015 [3], the majority of which were for the treatment of severe MR.

The mitral valve apparatus consists of an annulus from which the two leaflets emanate. Chordae tendineae arising from the free edge of each leaflet are attached

J. Brubert

to the papillary muscles of the left ventricle. Mitral regurgitation can arise from dysfunction of any of these components. Changes in the mitral valve, such as weakened leaflets and chordae, leads to primary mitral regurgitation and impaired systolic leaflet coaptation. In contrast, in secondary mitral regurgitation the mitral valve tissue is normal, but the supporting apparatus is altered. Generally, as the left ventricle becomes dilated and dyskinetic from ischemic or non-ischemic cardiomyopathies, the mitral valve leaflets fail to appose one another, leading to regurgitation [4]. In primary and secondary MR, systolic backflow of blood into the left atrium alters the ventricular pre-load and after-load. Initially these changes may be reversible, but with time irreversible decompensation occurs resulting in reduced contractility and symptoms of congestive heart failure. In primary MR the deterioration is gradual: 90% of the patients are alive at 8 years after diagnosis of MR, and 50% of these survive without any cardiac related events. In secondary MR, the intrinsic relationship between the mitral valve and left ventricle means that dysfunction of either structure begets further dysfunction such that transition is more rapid. Only 30% of patients survive to 5 years without a cardiac event [5].

Current solutions

Non-inotropic   and inotropic vasopressors, diuretics, vasodilators, and heart failure drugs have all been used to treat MR, but with no long term or reproducible success. As such, surgical intervention is the mainstay of treatment for MR. Given the complex nature of the mitral valve apparatus, various approaches are available to manage defects. The interaction between annulus, leaflets, chordae and ventricle has meant that complete valve replacement has been less successful, requires careful patient selection, and is generally avoided if possible. On the other hand, valve repair allows the dysfunctional portion of the valve apparatus to be corrected or

compensated for, typically by annuloplasty, leaflet resection, or neo-chordoplasty. The implantation of an annuloplasty ring is considered the gold standard for valve repair in functional/secondary MR, with a lower mortality rate, improved ventricular function, freedom from reoperation and anticoagulant complications, and superior long term survival than for replacement of the valve [6]. As such, repair is often the preferred intervention where possible.

Carpentier first introduced the mitral annuloplasty ring in 1969 as a means of re-shaping the annulus to improve leaflet coaptation [7]. The use of an undersized ring to reduce the annulus in secondary MR was first reported in 1995 [8]. Over this period, over 40 designs of mitral annuloplasty rings have been reported.

Currently, a variety of surgical annuloplasty ring devices are available: they can be classified as rigid or flexible, and planar or saddle-shaped. Some rings may be of an 'incomplete' C shape, extending around the posterior leaflet, and leaving a space across the base of the anterior leaflet. The physiological annulus is D-shaped when viewed axially and takes a saddle shape in 3-D space when loaded during systole. *In vivo*, *in vitro*, and *in silico* studies have suggested that augmenting the saddle form of the mitral valve annulus in a repair promotes optimum leaflet dynamics and reduces annular loading forces, promoting a more favorable outcome. While flexible rings may promote physiological dynamics, their lack of rigidity cannot provide the advantages conferred by a saddle form [9–11].

The benefits of patient specific shaping

Although mitral annuloplasty is superior to medical intervention and valve replacement, long term results after annuloplasty are still suboptimal, with recurrence of 2+ MR in 33% of the patients at 1 year, and 65% of the patients presenting with

recurrent MR at 2 years after surgery [12]. Current surgical mitral valve repair and replacement in severe ischemic MR carries a 20% mortality at 2 years. Among patients alive at 2 years following mitral valve repair, 60% have recurrent moderate or severe MR [13]. Undersized ring annuloplasty may unevenly displace the posterior annulus anteriorly, which leads to increased loading of the posterior leaflet [14]. Essentially, the mitral valve becomes functionally unileaflet. Leaflet tethering decreases leaflet curvature and results in increased leaflet and chordal stress [15]. Using saddle-shaped rings which are accurately sized to patients' mitral annulus directly affects the durability and effectiveness of mitral valve repairs [16]. Currently, a qualitative approach is taken to annuloplasty shaping and sizing. Advances in image acquisition allow high accuracy reconstructions of the mitral valve apparatus prior to intervention [9] and echocardiography and doppler allows repairs to be analyzed peri-operatively.

Proposed solution

We propose a mitral annuloplasty repair that is not fixed to a pre-set geometry, allowing peri-operative adjustment during the implantation procedure, and also post-operative adjustment. Such a device would allow an optimum repair to be achieved, and could allow readjustment to ameliorate the effects of ventricular remodeling. To achieve this, the REshapeable Mitral Annuloplasty DevIce (REMADI) consisting of a fully encapsulated low melting temperature alloy. The alloy is solid and rigid at body temperature and provides traction to shape the annulus. When heated, the alloy melts and the REMADI becomes malleable.

To enable the REMADI to be implanted percutaneously, attachment to the annulus is suture-less. We designed a set of anchors which automatically deploy when opposed to the tissue. Each anchor consists of two nickel titanium alloy barbs which

J. Brubert

become embedded in the annular tissue. Prior to deployment the barbs are constrained within a stainless-steel sheaf. Upon apposition to the tissue surface, the sheaf retracts allowing the barbs to return to their original, curved conformations. The barbs become embedded within the mitral valve annulus, thereby securing the annuloplasty ring.

There are several other devices for surgical, percutaneous or hybrid mitral valve repair which have been proposed, or have reached clinical testing. There is an array of devices of varying geometries, implantation methods, tissue attachment, and some with the facility to modify the geometry peri- or post-operatively; a selection of relevant devices are summarized in Table 1. While several of these devices have reached the first-in-man stage, there have been technical, clinical or commercial hurdles that have limited adoption. As a consequence, percutaneous repair of mitral regurgitation remains an unsolved problem.

Table 1 Summary of direct and indirect mitral annuloplasty devices.

Device	Features	Most recent status and reference or ClinicalTrials.gov identifier
Mitralign Bident (Mitralign)	Transventricular approach. Polyester pledglets for plication of the posterior annulus. No long-term adjustment.	Not in clinical use since CE mark trial [17]. Trial in tricuspid position NCT03016975.
Cardioband (Valtech/Edwards)	Transfemoral (transseptal) approach. Adjustable posterior rigid band. No long-term adjustment.	CE mark and 1 year trial [18]. Randomized controlled trial underway NCT03016975.
enCorSQ MVR system (MiCardia)	Surgical implantation. Nitinol ring with planar geometry. Postoperative transcatheter readjustment. Post-operative reduction to predetermined size.	CE mark [19].
Millipede ring (Millipede)	Transfemoral approach. Nitinol ring with pivoting	First in human [20], multi-center evaluation recruiting

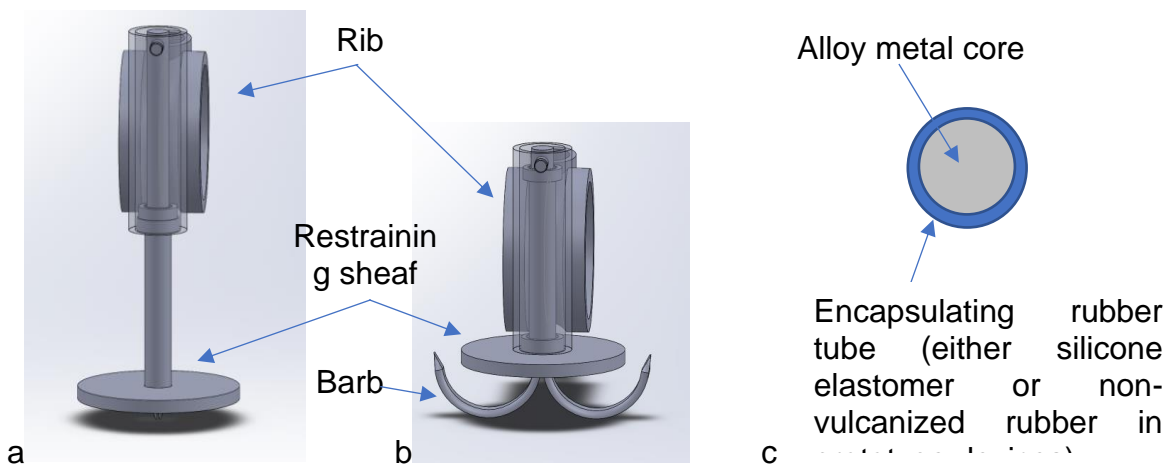|	anchors with planar circular geometry. No long-term adjustment.	NCT02607527
MitralFlex	Surgically implanted ring deformable by cable.	Animal feasibility study [21]
Amend ring (Valcare).	Transapical approach with expansion to a predetermined size. Rigid, planar, D-shaped ring. No long-term adjustment.	First in human [22].
n/a	Polycaprolactone ring with nickel–chromium alloy wire core, polyvinyl chloride tube coating, and polyester sewing cuff	Animal cadaver feasibility study [23]
Carillon (Cardiac Dimensions)	Indirect annuloplasty: Reshaping device placed in coronary sinus via venous access. Inconsistent relationship between coronary sinus and mitral valve.	Recruiting for multi-center randomized, double-blind trial is to assess the safety and efficacy (NCT03142152)

Methods

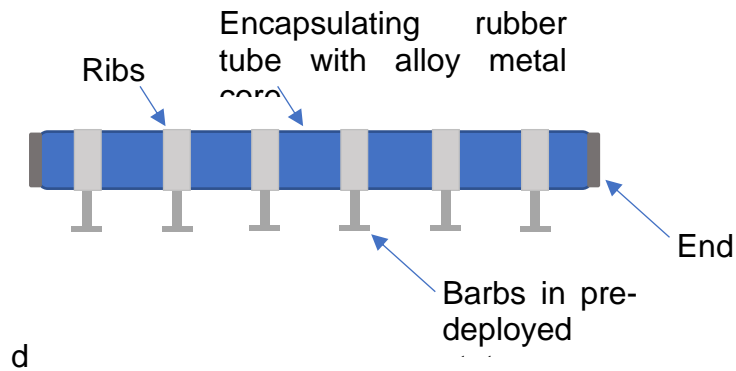### Annuloplasty ring manufacture

The annuloplasty ring is composed of a low melting temperature alloy core. A bismuth, indium, tin, zinc alloy (35, 48.6, 16, 0.4% weight respectively) was first proposed for biomedical uses in 2014 as a bone cement. The alloy melts at 57.5°C [24]. The encapsulating layer is a silicone elastomer MED-4420 (NuSil, Polymer Systems Technology Limited, UK). Appropriately sized rods were coated while rotating, before being cured in an environmental chamber at 50°C and 50% relative humidity for 24h.

Prototype devices used for testing were constructed using non-vulcanized latex rubber (MBFG, Ireland). Appropriately sized mandrels were dip coated in rubber solution before being rotated around their long axis, for a minimum of 24h. The rubber tubes were then released from the mandrel.

Attachment of the annuloplasty device to the annulus tissue is achieved using nitinol barbs, shown in Figure 1 a and b. The barbs were laser cut from nickel titanium wire in their straight (pre-deployed) conformation and shape set to their curved (deployed) form. The shaft of the barbs is secured within the anchor by a welded collar. The anchor is laser cut from 316L stainless steel and consists of a ring through which the annuloplasty tube passes. The barbs are welded to the outer surface of the ring. Another stainless-steel tube is welded to the inner surface of the ring and is used to engage the annuloplasty device with the delivery tool. Six anchors are evenly spaced along the length of the annuloplasty tube and bonded to the rubber encapsulating layer using cyanoacrylate.

The parts of the assembled device are illustrated in Figure 1 c and d. The rubber tube forms the encapsulating layer of the annuloplasty. The tubes were elongated by 200%, filled with molten alloy and then cooled while in this extended state. The ends of the rubber tubes were sealed using custom stoppers (FormLabs Tough Resin V2).

a   Rib   Restraining sheaf   Barb   b   c

Alloy metal core

Encapsulating rubber tube (either silicone elastomer or non-vulcanized rubber in

Ribs

Encapsulating rubber tube with alloy metal core

End

Barbs in pre-deployed

d

Figure 1 Schematic images of the annuloplasty and components. (a) Rib with anchor in pre deployed state, (b) rib with deployed anchor, (c) cross-section of annuloplasty ring, formed by injection filling of rubber tube with metal. (d) assembled device consisting of ring in a straight configuration with 6 ribs and barbs.

Delivery device manufacture

The prototype delivery tool was designed for in vitro catheter delivery. Six nitinol wires are used to form a basket. Axial compression of the nitinol wire members determines their radial displacement. Each member can be controlled individually, allowing non-circular shapes to be formed. The nitinol wires engage with the anchors of the annuloplasty device. The radial position of each spline can be controlled, and the axial position of each anchor with respect to each spline can be controlled, and as such any saddle form can be generated for the annuloplasty.

Tissue apposition testing

Engagement with the mitral annulus is achieved using the barbs. The force required to deploy and engage the barbs, and the force required to dehisce the barbs from the tissue were tested using a position controlled tensile tester (Texture Analyser, Stable Microsystems). Porcine hearts were obtained from a local abattoir and the mitral annulus dissected. The mitral annulus was restrained on the base plate using a Perspex sheet with a 10 mm hole through which the barb passed. Insertion and dehiscence were tested at a minimum of eight points on the atrial side of the mitral

annulus. The force required to dehisce the barbs from the tissue was compared with force required to dehisce a 2-0 monofilament suture from the mitral annulus.

Induction heating

Non-contact heating of the mitral annuloplasty was performed using an inductor (FlexHeat 2.0, RDO Induction, NJ, USA). In this feasibility study, induction heating was performed with an external coil around the left atrium and pulmonary vein, as illustrated in Figure 2. The induction heater is driven by a 2 kW power supply. The copper coil was internally cooled at a minimum flow rate of 2 $Lmin^{-1}$. The heater module is tuned to the resonant frequency of the coil and load. The alternating current through the coil induces an alternating magnetic field, which is strongest within the coil, where the annuloplasty device is located. The alternating magnetic field penetrates the conductive alloy core of the annuloplasty, inducing eddy currents which heat the metal core of the annuloplasty through joule heating. This is used peri-operatively to soften the device and alter it from a straight configuration for delivery, to a C-shape for implantation, and then for any fine adjustment of the saddle form. This configuration of induction heating coil is incompatible with in-vivo testing, but allows a minimum induction current to be used for feasibility testing. The final device would utilize an internal coil mounted on the delivery catheter.
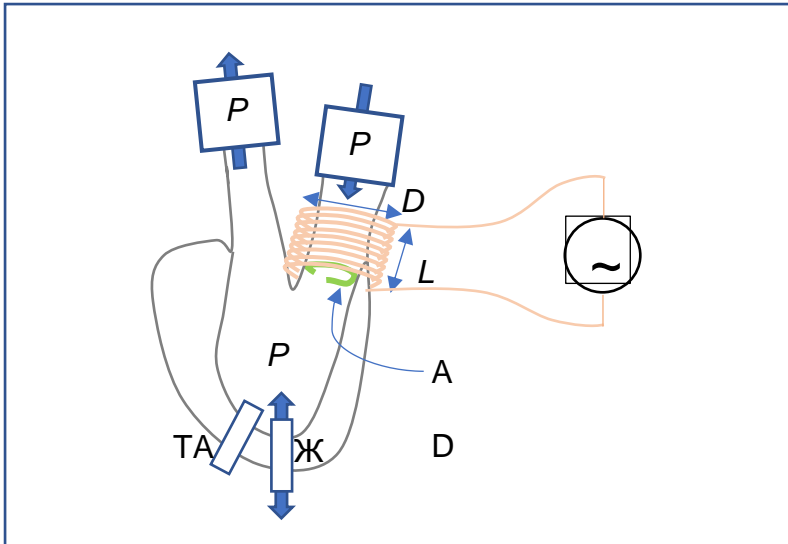
J. Brubert

Figure 2 Induction heating coil geometry for ex-vivo testing. Coil is formed from 9 turns of 1/8" copper tubing, with a length, L, of 34mm; diameter, D, of 30mm. P_1 indicates the upstream pressure, P_2 the ventricular pressure, P_3 the aortic root pressure. AD indicates the implanted annuloplasty device. The flow is driven using the apical port, Ж. TA indicates the transapical port through which the catheter and device is introduced.

Heat from the metal core of the annuloplasty ring will be dissipated through the encapsulating layer and into the environment.

Passive heart simulation

To test delivery and feasibility of the REMADI a porcine passive heart model was used [25] (Cardiac Biosimulator, LifeTec Group, Eindhoven, Netherlands). The passive heart model uses porcine hearts from a local abattoir. The hearts are frozen to reproduce their physiological mechanical properties. The hearts are mounted to the servo-controlled pump, in line with compliance and resistance modules to simulate pulsatile flow in the absence of active cardiac contraction. A port is placed at the apex, which provides the necessary pressure gradients to simulate diastolic and systolic flows through the heart. Without the requirement to pump blood, transparent fluids can be used, allowing direct endoscopic vision to be used.

J. Brubert

Absolute and transvalvular differential pressure measurements were taken during testing.

Results

Tissue apposition testing

The nitinol anchoring devices underwent *in vitro* testing to assess implantation and pullout force using a 2-0 polypropylene sutures as a control. A position-controlled tester implanted the anchors into a fresh porcine mitral annulus. Sample data from this experiment is shown in Figure 3. A single prototype anchor provided 2±0.5 N. The prototype device would be secured by a minimum of 6 anchors. Combined, the anchors would be sufficient to withstand the typical forces (1.2 ± 0.9N cyclic force, with a peak at 2.4 ± 4.5N) exerted upon a ring anchored in the mitral annulus under a systolic pressure 150 mmHg [26]. The 2-0 polypropylene suture provided at least 10 N.
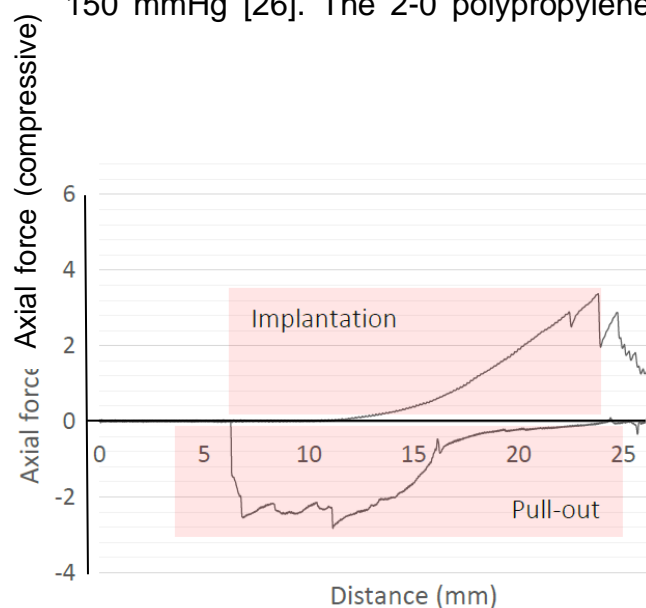
Figure 3 Sample prototype barb insertion and pull-out force (N) for a single nitinol barb. Distance is relative to the starting point of the barb, 11mm above the tissue.
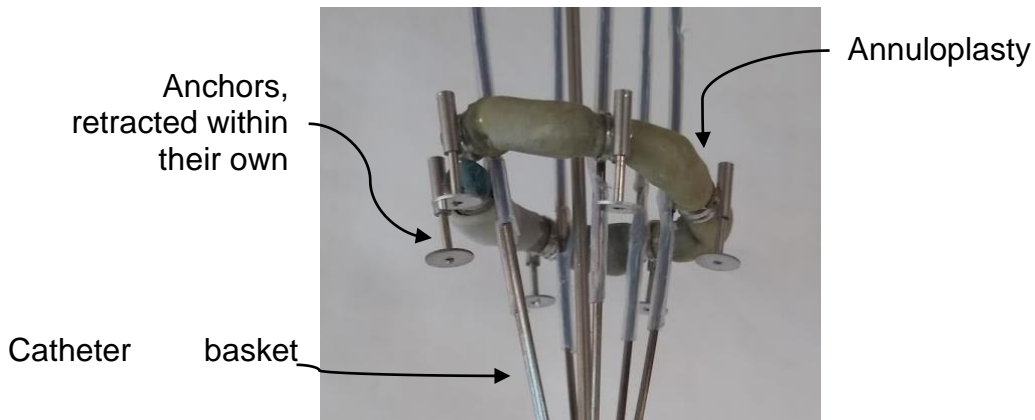
*Figure 4 REMADI mounted on the basket of the delivery catheter, with anchors in their pre-deployment state.*
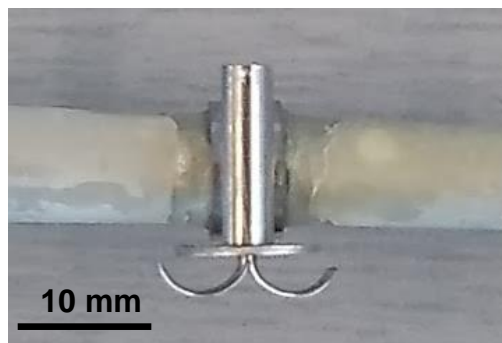
Figure 5 Nitinol anchor in deployed position.

Passive heart simulation

A proof-of-concept REMADI was assembled to demonstrate the feasibility of the REMADI. Complete reversibility of the soft-rigid state allowed the REMADI to be shaped to fit into a catheter, and shaped to the annulus once in the left atrium. For proof-of-concept a 32Fr catheter was used.

Four hearts were characterized on the passive heart platform. Gross and endoscopic images are shown in Figure 6 and Figure 7. Four implantations were performed. Three annuloplasties were implanted off-pump under direct vision with a trans atrial approach. One annuloplasty was implanted under simulated flow conditions using

the catheter delivery device through the apex of the left ventricle. There was an issue passing the chordae tendineae during the apical implantation, causing some damage. Figure 8 shows the ring being unsheathed within the left atrium. Once unsheathed, the induction heating system was used to soften the alloy core of the annuloplasty. The softened annuloplasty was then expanded using the basket, as shown in Figure 9. Retracting the annuloplasty device towards the apex brought the device into contact with the annulus. As the undeployed barbs make contact with the annulus, the restraining sheaths slide back into the device, allowing the barbs to become buried in the tissue of the annulus, as shown by the dissection image in Figure 11. With the REMADI attached to the annulus, the diameter of the device was reduced, and a saddle form produced.
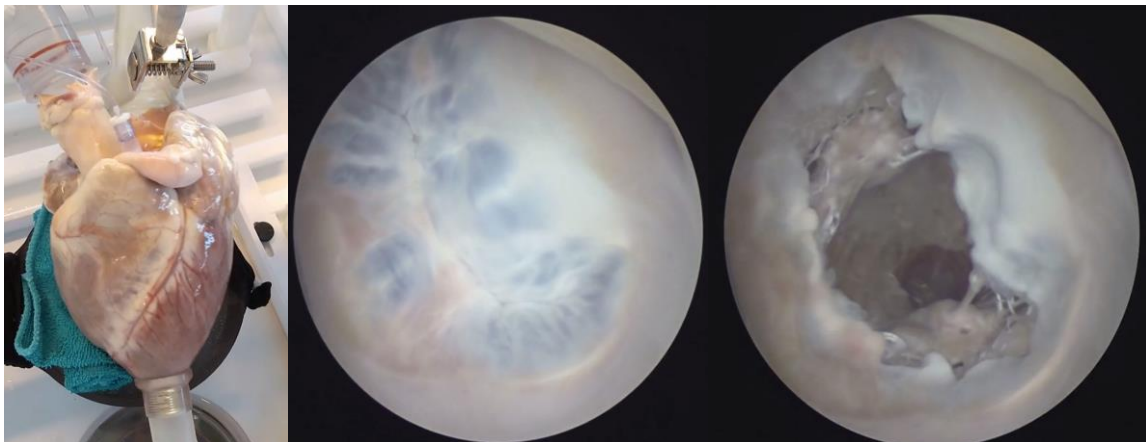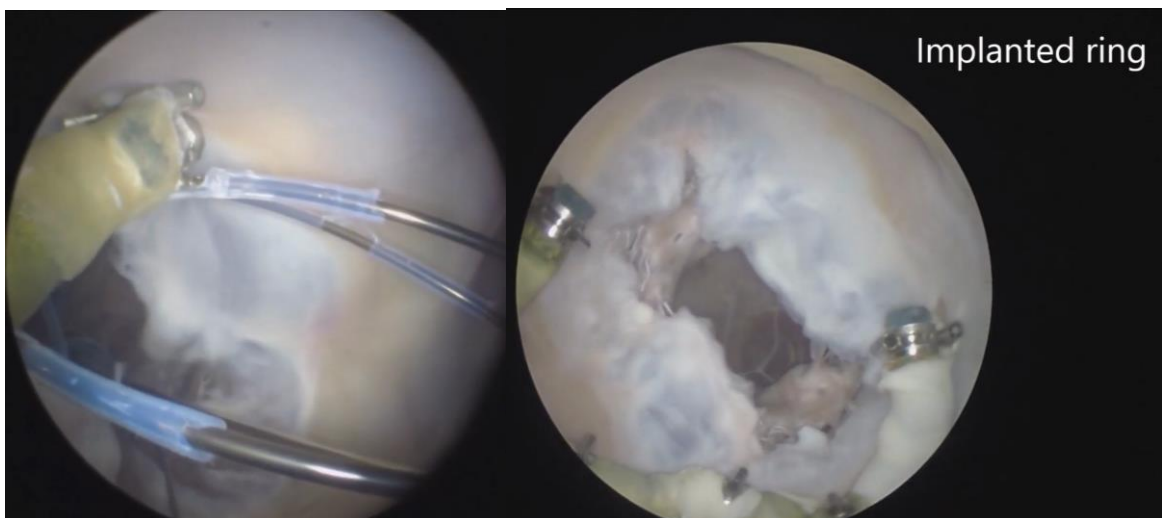

Figure 6 (l) passive beating heart simulator with pulmonary vein inflow, aortic outflow, and flow-driving apical port. Atrial view of mitral valve during systole (c) and diastole (r).
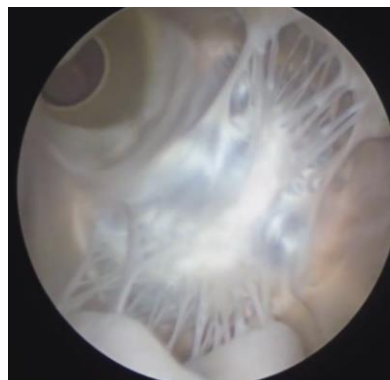
*Figure 7 Ventricular view of mitral and aortic valves during systole.*

Figure 8 Endoscopic view of unsheathing of the REMADI from the left atrium during systole (l) and diastole (r).

Figure 9 (L) With the REMADI in a softened state, the basket catheter can be expanded. (R) The ring engaged with the posterior annulus and disengaged from the delivery catheter.

The left atrial pressure, left ventricular pressure, and transvalvular pressure gradients are shown in Figure 10. The minor difference between the traces may reflect a change in valve dynamics induced by the ring, but given that the baseline was a healthy, not a lesion model, no change in hydrodynamics was sought. The regurgitant fraction could not be accurately measured on this setup as it was not

J. Brubert

possible to perform echocardiography, nor mount a high frequency ultrasonic flow probe on the pulmonary vein. Temperature probes placed in the annular tissue, and the left ventricle did not detect any change in temperature during heating.
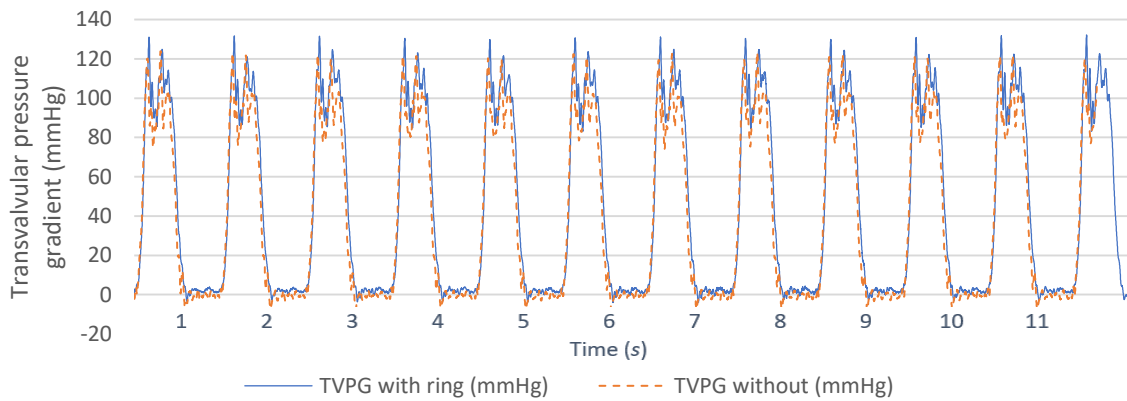
Figure 10 Transvalvular pressure gradient (TVPG) before and after implantation of an annuloplasty.

Figure 11 Benchtop dissection of heart demonstrating engagement of barbs with the annulus.

Discussion

The REMADI device tested in this study was designed to represent the key components required for an assessment of feasibility. In this regard, could the device be manufactured, fit into a delivery catheter, be transitioned to a soft state while in a

physiological flow (before and after engagement with the annulus), be shaped to a saddle form during delivery, engage with the mitral annulus, and provide a rigid deformation of the annulus.

The barb devices described and tested in this paper are a novel means of implanting an annuloplasty device. The absolute pull-out strength has been characterized, and is of an appropriate order of magnitude, however the effect of cyclic stress upon the engagement between the anchor and tissue has not been tested. Subsequent iterations of the REMADI would use a Dacron coating to promote full tissue integration into the mitral annulus. The design of the barbs of the anchors were optimized using linear estimates of the strain and stiffness. Finite element analysis may be used to optimize the dimensions of the barbs, whose dimensions are a critical factor for the overall profile of the device. A significant limitation of the barb method is the lack of control when deploying, and difficulty in retracting the barbs once deployed. The deployed barbs may be retracted, however this functionality is not built into the delivery device. Compared to the helical anchor method used by the Cardioband device [27], the REMADI anchors can be deployed more quickly.

There are several shortcomings to the delivery device used for implantation of the REMADI. The form of the basket delivery tool impinges upon the mitral valve and prevents the leaflets from closing during systole. As such, the open basket impeded closure of the mitral valve. Optimization of the basket wire shapes can reduce this limitation in future designs. The transapical route of delivery permits direct access to the mitral valve which is necessary for this delivery device. It also affords larger bore access, fewer closure related complications, and avoids atherosclerotic peripheral vessels, however it is perceived as being more invasive than transfemoral delivery [28]. Table 1 shows several direct annuloplasty devices which are delivered via a

J. Brubert

transseptal route with transfemoral access, which has become the first choice of implantation method for valves [29]. The option for transfemoral implantation would be preferred, and may ease adoption of the device.

In testing of the REMADI prototypes we encountered problems with the formation of cracks in the metal core upon re-freezing. To mitigate this issue the elastic encapsulating layer is overfilled, such that there is a positive pressure on the metal core. This is achieved by filling the encapsulating tube in an elongated state. Furthermore, the starting length of the encapsulating tube is less than the minimum desirable circumference of the mitral annulus; the device is stretched in order to engage with the mitral annulus before the remodeling step reduces both the device length and the annulus diameter.

The effects of heating the device upon the surrounding tissues were a significant consideration in the design of the REMADI. While the core reaches temperatures in excess of 60°C, the encapsulating layer insulates the environment. The degree of insulation is limited by the thickness and thermomechanical properties of the material. The flow of blood past the device rapidly dissipates heat from the device. The assays that we have performed thus far have not been sensitive enough to detect any hemolysis or coagulation from this heating effect. The effects of relatively short contact times with relatively mild temperature increases have received little attention in the literature. Seki *et al.*, 2018 also tested the effects of heating a mitral annuloplasty, albeit to 40°C, with no indication of necrosis. The use of induction heating is not a common procedure, but there is precedence in the field: the enCorSQ MVR system (MiCardia) device uses induction to activate a phase change in nitinol [19]. The frequency of the inductor can be tuned to ensure maximum

energy transfer to the metal core. The penetration depth of the alternating magnetic field can be calculated from:

$$\delta = \frac{1}{\sqrt{\pi f \mu \sigma}}$$

where δ is the penetration depth (m), f is the frequency (Hz), μ is the magnetic permeability of the material (H/m), and σ is the electrical conductivity of the material (S/m). When the penetration depth exceeds the thickness of the material, eddy currents are not generated and there is minimal energy transfer. As such, smaller metal components such as the barbs, are not heated.

Although the core of the REMADI does not make contact with any biological elements, nonetheless the material has been tested for its hemo- and biocompatibility, which are sufficient for long term implantation in accordance with ISO 10993 and published in [24]. The encapsulating layer is an elastomeric silicone material with ISO 10993 compliance for long term implantation in blood contacting devices.

In this paper we demonstrated that the shape of the REMADI can be altered after implantation. As such, the REMADI could potentially accept a transcatheter mitral valve implantation (TMVI). Transitioning the prosthesis to a soft state allows the REMADI to conform to the perimeter of the valve implant, minimizing paravalvular leak and uneven TMVI expansion which may occur with rigid annuloplasty devices. The valve-in-ring concept emulates the accepted clinical pathway of transcatheter aortic valve implant (TAVI)-in-valve [30]. The second benefit of post-operative adjustment of a mitral annuloplasty ring is to reshape the annulus in a controlled

fashion to eliminate any subsequent recurrent mitral regurgitation, this has not been demonstrated in this paper, and requires the catheter to reengage with the device.

Peri-operative adjustment of the mitral annuloplasty ring allows for patient specific optimization of the repair. The exact MR phenotype takes a different form in every patient [9], as such the ability to perform a patient specific annuloplasty (with peri-operative feedback) may be of significant benefit. Carpentier described an optimal repair as (1) preserving or restoring full leaflet motion, (2) creating a large surface of coaptation, and (3) to remodeling and stabilizing the entire annulus [31]. Points (1) and (2) may be altered by manipulation of the annuloplasty ring after implantation which can be evaluated using peri-operative echocardiography. As such, the REMADI may confer a benefit over the other devices proposed elsewhere, as summarized in Table 1, which are not capable of long term adjustment and may only be adjusted to a pre-determined size.

To complete testing of the REMADI, and demonstrate its effectiveness, further testing is warranted in a MR lesion model, both *in vitro* and *in vivo*. Finally, assessment of the durability of the REMADI and its components requires further evaluation.

Conclusion

The REMADI is a novel device for the treatment of mitral regurgitation with the capability to be reshaped peri-operatively to achieve an optimal saddle shaped conformation, and post-operatively to accept a transcatheter mitral valve. It may also be capable of post-operative adjustment to correct any future MR recurrence as a result of ventricular remodelling. The solid-liquid phase transition of a low melting temperature alloy is used to achieve a soft and rigid state allowing the device to fit

within a catheter, as well as adopt any required mitral annulus form. The nitinol anchor system has demonstrated feasibility to engage with mitral annular tissue and secure a device. The prototype REMADI was constructed, and then tested in a beating heart model where the annulus could be deformed by the device.

Acknowledgements

Bibliography

[1]   Iung, B., and Vahanian, A., 2011, "Epidemiology of Valvular Heart Disease in the Adult.," Nat. Rev. Cardiol., **8**(3), pp. 162–172.

[2]   Enriquez-sarano, M., Akins, C. W., and Vahanian, A., 2009, "Mitral Regurgitation," Lancet, **373**(9672), pp. 1382–1394.

[3]   The Society for Cardiothoracic Surgery in Great Britain & Ireland, 2015, *The Blue Book*.

[4]   Espiritu, D., Onohara, D., Karla, K., Sarin, E., and Padala, M., 2016, "Transcatheter Mitral Valve Repair Therapies : Evolution, Status and Challenges," Ann. Biomed. Eng.

[5]   Grigioni, F., Detaint, D., Avierinos, J. F., Scott, C., Tajik, J., and Enriquez-Sarano, M., 2005, "Contribution of Ischemic Mitral Regurgitation to Congestive Heart Failure after Myocardial Infarction," J. Am. Coll. Cardiol., **45**(2), pp. 260–267.

[6]   Gammie, J. S., Sheng, S., Griffith, B. P., Peterson, E. D., Rankin, J. S., O'Brien, S. M., and Brown, J. M., 2009, "Trends in Mitral Valve Surgery in the

United States: Results From The Society of Thoracic Surgeons Adult Cardiac Database," Ann. Thorac. Surg., **87**(5), pp. 1431–1439.

[7]   Carpentier, A., 1969, "Reconstructive Valvuloplasty. A New Technique of Mitral Valvuloplasty," Presse Med., **77**(7), pp. 251–3.

[8]   Bach, D. S., and Bolling, S. F., 1995, "Early Improvement in Congestive Heart Failure after Correction of Secondary Mitral Regurgitation in End-Stage Cardiomyopathy," Am. Heart J., **129**(6), pp. 1165–1170.

[9]   Drach, A., Khalighi, A. H., and Sacks, M. S., 2018, "A Comprehensive Pipeline for Multi - Resolution Modeling of the Mitral Valve: Validation, Computational Efficiency, and Predictive Capability," Int. J. Numer. Methods Biomed. Eng., **34**, pp. 1–30.

[10] Mahmood, F., Iii, J. H. G., Subramaniam, B., Gorman, R. C., Panzica, P. J., Hagberg, R. C., Lerner, A. B., Hess, P. E., Maslow, A., and Khabbaz, K. R., 2010, "Changes in Mitral Valve Annular Geometry After Repair: Saddle-Shaped Versus Flat Annuloplasty," ATS, **90**(4), pp. 1212–1220.

[11] Ryomoto, M., and Mitsuno, M., 2014, "Is Physiologic Annular Dynamics Preserved After Mitral Valve Repair With Rigid or Semirigid Ring ?," Ann. Thorac. Surg., **97**(2), pp. 492–497.

[12] Acker, M. A., Dagenais, F., Goldstein, D., Kron, I. L., and Perrault, L. P., 2015, "Severe Ischemic Mitral Regurgitation: Repair or Replace?," J. Thorac. Cardiovasc. Surg., **150**(6), pp. 1425–1427.

[13] Goldstein, D., Moskowitz, A. J., Gelijns, A. C., Ailawadi, G., Parides, M. K., Perrault, L. P., Hung, J. W., Voisine, P., Dagenais, F., Gillinov, A. M., Thourani, V., Argenziano, M., Gammie, J. S., Mack, M., Demers, P., Atluri, P., Rose, E. A., O'Sullivan, K., Williams, D. L., Bagiella, E., Michler, R. E., Weisel, R. D., Miller, M. A., Geller, N. L., Taddei-Peters, W. C., Smith, P. K., Moquete, E., Overbey, J. R., Kron, I. L., O'Gara, P. T., and Acker, M. A., 2015, "Two-Year Outcomes of Surgical Treatment of Severe Ischemic Mitral Regurgitation," N. Engl. J. Med., **374**(4), pp. 344–353.

[14] Kuwahara, E., Otsuji, Y., Iguro, Y., Ueno, T., Zhu, F., Mizukami, N., Kubota, K.,

Nakashiki, K., Yuasa, T., Yu, B., Uemura, T., Takasaki, K., Miyata, M., Hamasaki, S., Kisanuki, A., Levine, R. A., Sakata, R., and Tei, C., 2006, "Mechanism of Recurrent/Persistent Ischemic/Functional Mitral Regurgitation in the Chronic Phase after Surgical Annuloplasty: Importance of Augmented Posterior Leaflet Tethering," Circulation, **114**(SUPPL. 1).

[15] Salgo, I. S., Gorman, J. H., Gorman, R. C., Jackson, B. M., Bowen, F. W., Plappert, T., St John Sutton, M. G., and Edmunds, L. H., 2002, "Effect of Annular Shape on Leaflet Curvature in Reducing Mitral Leaflet Stress," Circulation, **106**(6), pp. 711–717.

[16] Bouma, W., Aoki, C., Vergnat, M., Pouch, A., Sprinkle, S., Gillespie, M., Mariani, M., Jackson, B., Gorman, R., and Gorman, J. H. I., 2015, "Saddle-Shaped Annuloplasty Improves Leaflet Coaptation in Repair for Ischemic Mitral Regurgitation," Ann. Thorac. Surg., **100**(4), pp. 1360–1366.

[17] Nickenig, G., and Hammerstingl, C., 2015, "The Mitralign Transcatheter Direct Mitral Valve Annuloplasty System," Eurointervention, **11**, pp. W62–W63.

[18] Messika-Zeitoun, D., Nickenig, G., Latib, A., Kuck, K.-H., Baldus, S., Schueler, R., La Canna, G., Agricola, E., Kreidel, F., Huntgeburth, M., Zuber, M., Verta, P., Grayburn, P., Vahanian, A., and Maisano, F., 2018, "Transcatheter Mitral Valve Repair for Functional Mitral Regurgitation Using the Cardioband System: 1 Year Outcomes," Eur. Heart J., **40**(5), pp. 466–472.

[19] Langer, F., Borger, M. A., Czesla, M., Shannon, F. L., Sakwa, M., Doll, N., Cremer, J. T., Mohr, F. W., and Schäfers, H. J., 2013, "Dynamic Annuloplasty for Mitral Regurgitation," J. Thorac. Cardiovasc. Surg., **145**(2), pp. 425–429.

[20] Lashinski, R. T., Rust, M., Macaulay, P., Daniels, T. W., and Kristoffersen, K., 2016, "Method of Reconfiguring a Mitral Valve Annulus," p. 68.

[21] Tozzi, P., Locca, D., Gronchi, F., Hayoz, D., Ferrari, E., von Segesser, L. K., and Hullin, R., 2013, "Active Mitral Ring for Post-Surgical Remote Correction of Residual Mitral Regurgitation on the Beating Heart," Eur. J. Cardio-thoracic Surg., **44**(2), pp. 370–374.

[22] Taramasso, M., and Latib, A., 2016, "Percutaneous Mitral Annuloplasty,"

Interv. Cardiol. Clin., **5**(1), pp. 101–107.

[23] Seki, T., Jimuro, K., Shingu, Y., Wakasa, S., Katoh, H., Ooka, T., Tachibana, T., Kubota, S., Ohashi, T., and Matsui, Y., 2018, "Mechanical Properties of a New Thermally Deformable Mitral Valve Annuloplasty Ring and Its Effects on the Mitral Valve," J. Artif. Organs, **0**(0), p. 0.

[24] Yi, L., Jin, C., Wang, L., and Liu, J., 2014, "Liquid-Solid Phase Transition Alloy as Reversible and Rapid Molding Bone Cement.," Biomaterials, **35**(37), pp. 9789–801.

[25] Leopaldi, A. M., Vismara, R., Tuijl, S. Van, Redaelli, A., Vosse, F. N. Van De, Fiore, G. B., and Rutten, M. C. M., 2015, "A Novel Passive Left Heart Platform for Device Testing and Research," Med. Eng. Phys., **37**(4), pp. 361–366.

[26] Siefert, A. W., Pierce, E. L., Lee, M., Jensen, M. Ø., Aoki, C., Takebayashi, S., Fernandez Esmerats, J., Gorman, R. C., Gorman, J. H., and Yoganathan, A. P., 2014, "Suture Forces in Undersized Mitral Annuloplasty: Novel Device and Measurements.," Ann. Thorac. Surg., **98**(1), pp. 305–9.

[27] Taramasso, M., Guidotti, A., Cesarovic, N., Denti, P., Addis, A., Candreva, A., Nietlispach, F., Fleischmann, T., Emmert, M. Y., and Maisano, F., 2016, "Transcatheter Direct Mitral Annuloplasty with Cardioband : Feasibility and Efficacy Trial in an Acute Preclinical Model," Eurointervention, **12**, pp. 1428–1434.

[28] Walther, T., and Kempfert, J., 2012, "Transapical vs. Transfemoral Aortic Valve Implantation: Which Approach for Which Patient, from a Surgeon's Standpoint," Ann. Cardiothorac. Surg., **1**(2), pp. 216–219.

[29] Bleiziffer, S., Krane, M., Deutsch, M. A., Elhmidi, Y., Piazza, N., Voss, B., and Lange, R., 2013, "Which Way in? The Necessity of Multiple Approaches to Transcatheter Valve Therapy," Curr. Cardiol. Rev., **9**, pp. 268–273.

[30] Milburn, K., Bapat, V., and Thomas, M., 2014, "Valve-in-Valve Implantations: Is This the New Standard for Degenerated Bioprostheses? Review of the Literature," Clin. Res. Cardiol., **103**(6), pp. 417–429.

[31] Carpentier, A., Adams, D., and Filsoufi, F., 2010, *Carpentier's Reconstructive*

Valve Surgery, Saunders, Philadelphia.

J. Brubert

Figure 1 Schematic images of the annuloplasty and components. (a) Rib with anchor in pre deployed state, (b) rib with deployed anchor, (c) cross-section of annuloplasty ring, formed by injection filling of rubber tube with metal. (d) assembled device consisting of ring in a straight configuration with 6 ribs and barbs.

Figure 2 Induction heating coil geometry for ex-vivo testing. Coil is formed from 9 turns of 1/8" copper tubing, with a length, L, of 34mm; diameter, D, of 30mm. P_1 indicates the upstream pressure, P_2 the ventricular pressure, P_3 the aortic root pressure. AD indicates the implanted annuloplasty device. The flow is driven using the apical port, Ж. TA indicates the transapical port through which the catheter and device is introduced.

Figure 3 Sample prototype barb insertion and pull-out force (N) for a single nitinol barb. Distance is relative to the starting point of the barb, 11mm above the tissue.

Figure 4 REMADI mounted on the basket of the delivery catheter, with anchors in their pre-deployment state.

Figure 5 Nitinol anchor in deployed position.

Figure 6 (l) passive beating heart simulator with pulmonary vein inflow, aortic outflow, and flow-driving apical port. Atrial view of mitral valve during systole (c) and diastole (r).

Figure 7 Ventricular view of mitral and aortic valves during systole.

Figure 8 Endoscopic view of unsheathing of the REMADI from the left atrium during systole (l) and diastole (r).

Figure 9 (L) With the REMADI in a softened state, the basket catheter can be expanded. (R) The ring engaged with the posterior annulus and disengaged from the delivery catheter.

Figure 10 Transvalvular pressure gradient (TVPG) before and after implantation of an annuloplasty.

Figure 11 Benchtop dissection of heart demonstrating engagement of barbs with the annulus.

Table 1 Summary of direct and indirect mitral annuloplasty devices.

J. Brubert